UDK 69.036.03

***Gaponova L.V.***, *PhD, Associate Professor*
*ORCID 0000-0002-1326-0595 Gaponova.lyudochka@bk.ru*
***Grebenchuk S.S.***, *post-graduate*
*moisei2529@mail.ru*
*O.M. Beketov National University of Urban Economy in Kharkov*

# STRESS AND STRAIN BEHAVIOUR OF REINFORCED CONCRETE ANISOTROPIC SHELLS

*The character changes deflected mode of «Monofant» system fragments. For experimental studies state snippets new structural system of "Monofant" multi conformity was deformed and method based on hydrostatic load when the load is given by the weight of water, was used, and its value is governed by the height of the water column. To determine the qualitative and quantitative research object deformation measurements displacement cylindrical and spherical shells in 25 points was carried. However, the configuration structure complexity was given, which in turn led to the emergence of both vertical and horizontal movements of the studied surface shell under vertical load, the need to measure movements in two directions in a cylindrical shell of vertical displacement and a spherical shell. The study shows that the structural elements are endowed with all the necessary strength characteristics and attributes rigidity bearing elements of reinforced concrete buildings.*

***Key words:*** *stress-strain state, strain, envelope, reinforced concrete, experimental research.*

***Гапонова Л.В.***, *к.т.н., доцент*
***Гребенчук С.С.***, *аспірант*
*Харківський національний університет міського господарства імені О.М. Бекетова*

# НАПРУЖЕНО-ДЕФОРМОВАНИЙ СТАН ЗАЛІЗОБЕТОННИХ АНІЗОТРОПНИХ ОБОЛОНОК

*Досліджено характер зміни напружено-деформованого стану фрагментів системи «Монофант». Для експериментальних досліджень деформованого стану фрагментів нової конструктивної системи багатокритеріального призначення «Монофант» використано метод, заснований на гідростатичному навантаженні, коли воно задається вагою води, і її величина регулюється висотою водяного стовпа. Для визначення якісного та кількісного характеру деформування об'єкта дослідження здійснено виміри переміщень циліндричної і сферичної оболонок у 25-ти точках. При цьому з огляду на складність конфігурації конструкцій, що у свою чергу зумовило появу як вертикальних, так і горизонтальних переміщень досліджуваної поверхні оболонки під дією вертикального навантаження, виникла необхідність вимірювання переміщень у двох напрямках у циліндричній оболонці й вертикальних переміщень в сферичної оболонці. З проведеного дослідження випливає, що конструктивні елементи наділено всіма необхідними характеристиками міцності та жорсткісними атрибутами несучих елементів будівель з монолітного залізобетону.*

***Ключові слова:*** *напружено-деформований стан, переміщення, оболонка, залізобетон, експериментальні дослідження.*

**Introduction**. Building structures own weight minimizing is one of the most important trends in researching and enhancing construction options with limited resources. A new construction system named «Monofant» [1] was developed by scientific efforts of the building structure department of O.M. Beketov NUUE.

Using the large scale sheet blockouts of expanded polystyrene and mineral rock wool significantly decreases building cost and enhances its thermal and sound insulation parameters. Making the shells by the wet shotcreting method is the special feature of «Monofant» spatial curved structures [2]. The formed structure saves concrete (up to 40-45%) and provides slight saving of reinforcing bars as well.

In this case the shape and dimensions of created internal cavities drastically influences on the character of stress and strains conduct of the system.

**Analysis of recent research sources and publications.** The research objects are fragments of cylindrical/ spherical shells of the «Monofant» system of plan dimensions 2200×2200 mm. Each fragment is made of 50 mm thick external/ internal concrete coatings and 160 mm permanent blockout of expanded polystyrene inserted between them. Coating reinforcement is done with grid of 200×200 mm mesh, and d = 6 mm (A-I). The 50 mm ribs providing combined operation of shells are arranged in diagonal direction of the shell. The ribs are reinforced with flat frame of d = 10 mm (A-I). The general diagram of structures is given in fig. 1 -- 2.

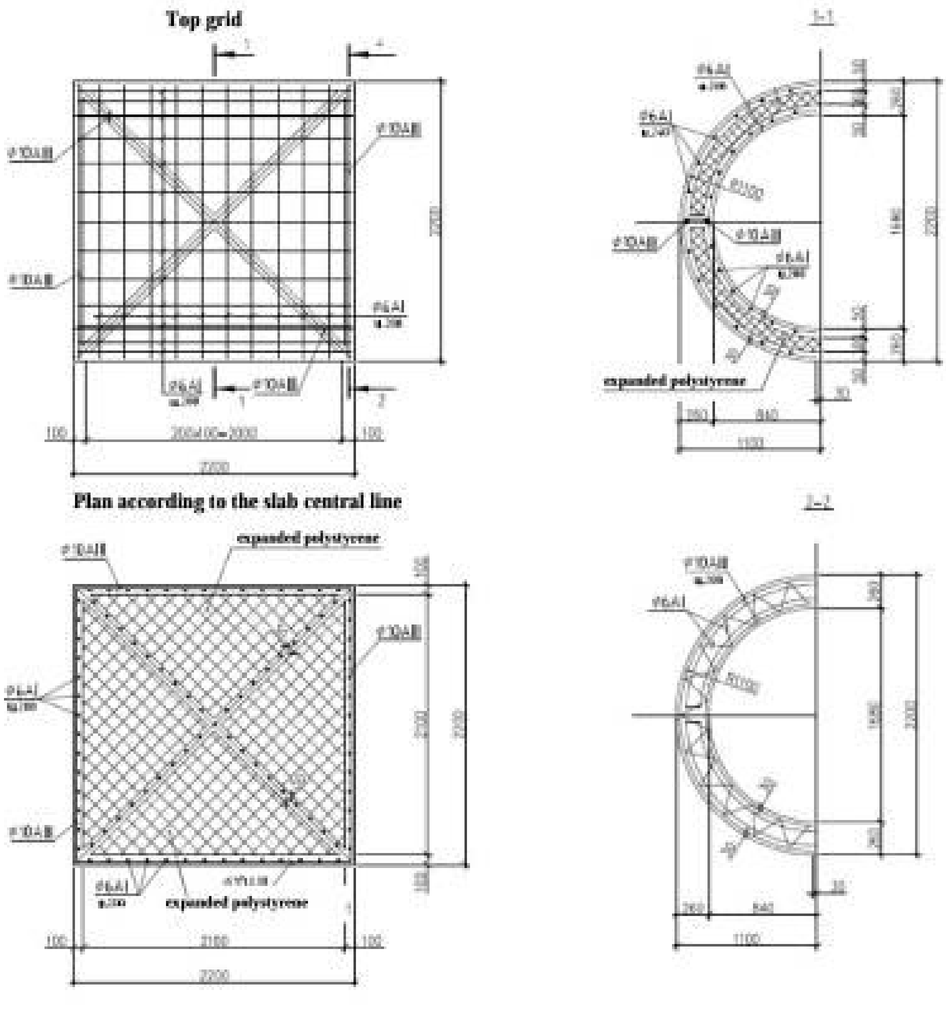


**Figure 1 – The geometry and reinforcement of the cylindrical shell**

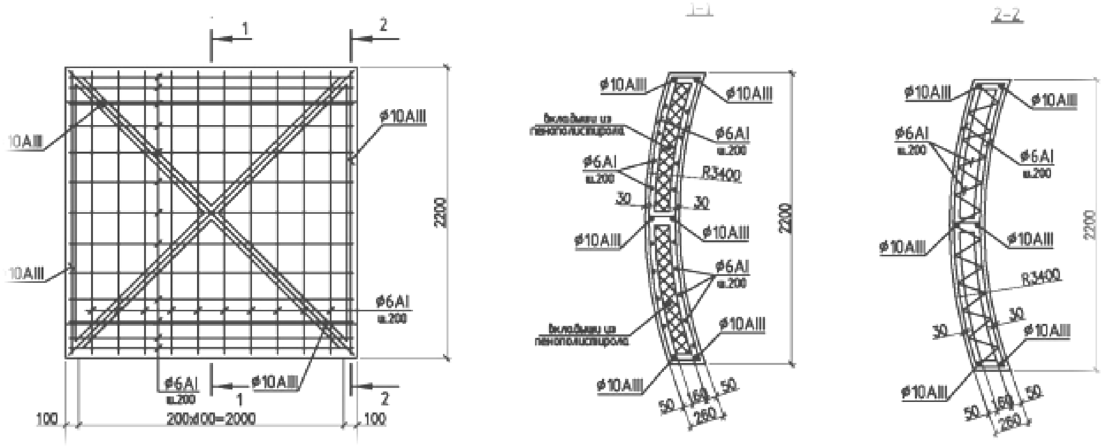


**Figure 2 – The geometry and reinforcement of the spherical shell**

**Main part of the research and obtained results.** A finite element model of the developed shell was built in the «ANSYS» software within the research.

The toolset of the mentioned calculation package allows to carry out the automatic triangulation of complex shapes into finite volumetric elements through the automatic import from additional software package of 3D modeling (in this case «Autodesk Inventor» was used). (fig. 3, 4).

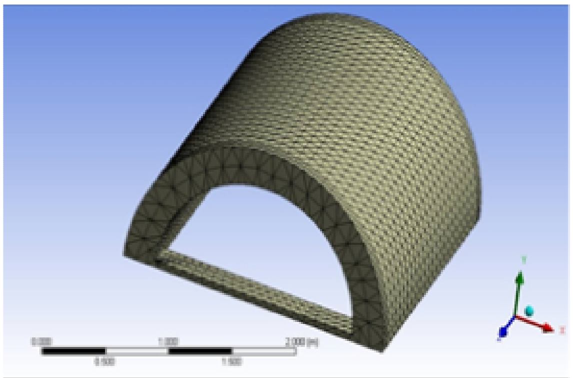

**Figure 3 – Building a cylindrical shell finite element grid**

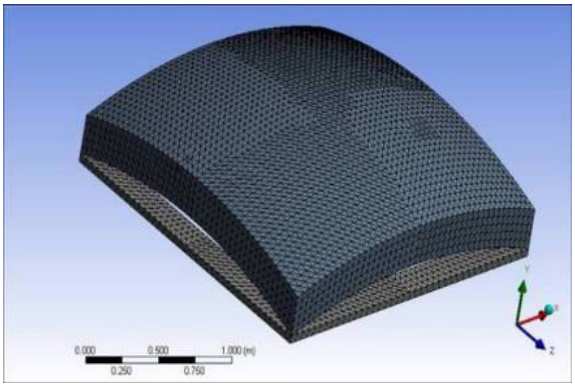

**Figure4 –shell finite element model**

The built cylindrical shell model contains 209,319 assemblies and 100,271 finite elements, whereas the built spherical shell contains 459,061 elements and 261,791 assemblies.

Resting was chosen as swiveling and fixed on four angular points of the shell in the plan.

Evenly distributed load was applied to the shell surface according to diagrams described in papers [3, 4]. Taking into account the structure rigidness, the evenly distributed load value made 10 kN/m$^2$. Once a stress-strain behavior theoretical analysis of a spherical shell fragment had been completed, experiment series on fabricated elements followed.

**Basic material and results.** The completed theoretical analysis [4, 5] is supported by experimental researches of new «Monofant» structural system fragments strained state against many criteria and by the hydrostatic method.

***Loading system***. In the research the method based on hydrostatic loading was used, when the load was created by water mass and its value was controlled by height of water column.

The loading mode was chosen according to an experiment program. Loading level was defined by height of water in the pool. In this case the mentioned level was provided by water supply/ drainage system to/ from the pool. To register measured movements of the studied object, series of dial indicators was installed; they allowed to measure stress-strain features of the studied object. A device to test slabs and shells in situ under influence of vertical short/long time loads was chosen as a basis for the mentioned tests.

The device contained the studied structure 1, installed on supports 2, boards 3 that created a tank, being installed along the contour of the loaded area, waterproof film 4 inside the tank, supplying/ draining hoses 5. Such structure is simple, cheap, and easy matching with the measurement system.

Considering the difficult configuration of the loaded shell surface, and in order to evenly distribute the water column pressure, the arrangement of additional partitions inside the pool in the longitudinal direction was considered as necessary. Therefore, the pool constructed over the spherical shell was a cell system consisting of 121 cells with dimension of 200×200 mm and height of 1200 mm (fig.5).

Pool walls and internal partitions were made of 20 mm thick multilayer glued plywood (fig. 6). The pool constructed over the cylindrical shell was a cell system consisting of 11 cells with dimension of 200×2200 mm and height of 1200 mm.

Pool walls and internal partitions were made of 20 mm thick multilayer glued plywood (fig. 7, 8).

**Figure 5 – A general view of the cell pool to test the spherical shell**

**Figure 6 – The cell system over the shell**

**Figure 7 – The cell system over the cylindrical shell to carry out tests**

**Figure 8 – Boards forming a pool over the cylindrical shell**

The pool external walls rested on the frame, whereas the internal partitions were rigidly attached to the external walls by glue and self-tappers. 10 mm space was arranged between the pool internal partitions and the shell. The space was filled with expanding foam to distribute the pool own mass over the frame only. Specifically fabricated plastic pockets were installed in each formed cell. It provided pool impermeability.

***Measurement system***. To define qualitative and quantitative features of studied object straining, shell movement measurement were done in 25 points. In this case, considering the complexity of the structure, that in its turn had preconditioned the occurrence of both vertical and horizontal movements of the studied shell surface under the vertical load effect, the necessity of measuring 2 direction movements (fig. 9) in the cylindrical shell and vertical movements in the spherical shell emerged (fig. 10).

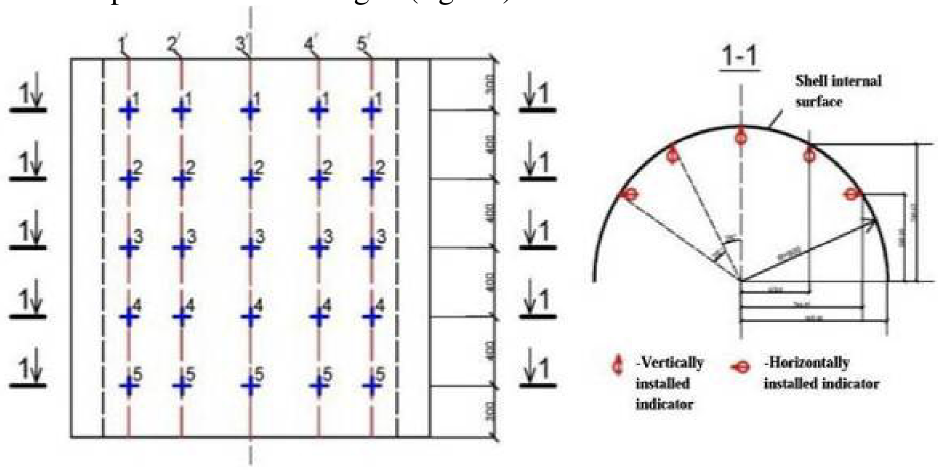


**Figure 9 – A diagram of indicator installation in the cylindrical shell**

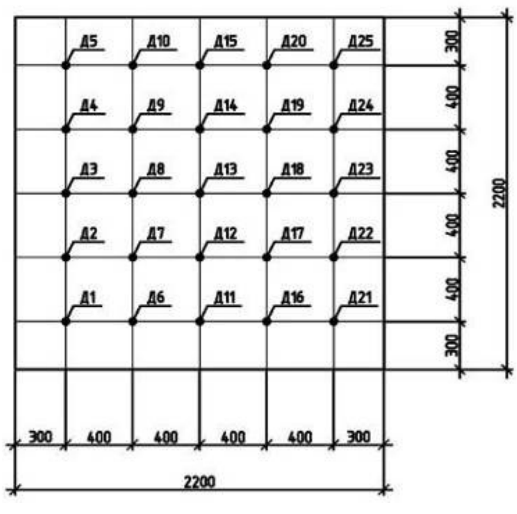


**Figure 10 – A diagram of indicator installation in the spherical shell**

Besides, considering the shell significant rigidity, which had preconditioned the smallness of the expected movement values, dial indicators with 2 um division value and 2 mm rod travel were used. The indicators were fastened in the indicated points by specifically fabricated frames made of 40×3 mm square pipes and 10×10 mm metal bar (fig. 11) that in their turn were welded to the main frame. Sequence of experiments is illustrated in fig. 12 -- 16.

Six independent cycles of loading/ unloading were done according to each loading diagram. Averaged data of six loading results were analyzed. The data are given in the table 1 – 2.

**Figure 11 – Measurement system**

**Figure 12 – Filling the cells with water**

**Figure 13 – Adjusting a water level in cells**

**Figure 14 – A cell filled with water**

**Figure 15 – Cells filled with water**


**Figure 16 – The bench to carry out tests**

**Table 1 – Averaged readings of vertical movement indicators of the cylindrical shell**

| Indicator | Vertical movements, absolute values (mm) | | | | | |
|---|---|---|---|---|---|---|
| | Full loading | Δ | 1/2 of the surface | Δ | 1/3 of the surface | Δ |
| 1'1 | 0,041 | -0,007 | 0,01 | 0,007 | 0,024 | -0,016 |
| 1'2 | 0,138 | -0,006 | 0,062 | -0,008 | 0,053 | -0,007 |
| 1'3 | 0,228 | -0,01 | 0,112 | -0,015 | 0,086 | -0,006 |
| 1'4 | 0,138 | -0,006 | 0,062 | -0,008 | 0,053 | -0,001 |
| 1'5 | 0,041 | -0,007 | 0,01 | 0,007 | 0,024 | -0,016 |
| 2'1 | 0,012 | -0,004 | 0,055 | 0,006 | 0,045 | 0,005 |
| 2'2 | 0,194 | -0,007 | 0,069 | 0,0 | 0,056 | 0,0 |
| 2'3 | 0,237 | -0,004 | 0,078 | -0,011 | 0,063 | -0,004 |
| 2'4 | 0,194 | -0,007 | 0,069 | 0,0 | 0,056 | 0,0 |
| 2'5 | 0,012 | -0,004 | 0,055 | 0,006 | 0,045 | 0,005 |
| 3'1 | 0,197 | -0,003 | 0,098 | 0,007 | 0,081 | 0,007 |
| 3'2 | 0,217 | -0,004 | 0,105 | -0,001 | 0,086 | -0,008 |
| 3'3 | 0,242 | -0,013 | 0,117 | -0,01 | 0,092 | 0,004 |
| 3'4 | 0,217 | -0,004 | 0,105 | -0,001 | 0,086 | -0,008 |
| 3'5 | 0,197 | -0,003 | 0,098 | 0,007 | 0,081 | 0,007 |
| 4'1 | 0,012 | -0,004 | 0,166 | 0,005 | 0,131 | 0,005 |
| 4'2 | 0,194 | -0,007 | 0,178 | 0,0 | 0,148 | -0,006 |
| 4'3 | 0,237 | -0,004 | 0,192 | -0,011 | 0,157 | -0,005 |
| 4'4 | 0,194 | -0,007 | 0,178 | 0,0 | 0,148 | -0,006 |
| 4'5 | 0,012 | -0,004 | 0,166 | 0,005 | 0,131 | 0,005 |
| 5'1 | 0,041 | -0,007 | 0,088 | -0,012 | 0,088 | -0,002 |
| 5'2 | 0,138 | -0,006 | 0,102 | -0,006 | 0,093 | -0,007 |
| 5'3 | 0,228 | -0,01 | 0,121 | -0,005 | 0,111 | -0,004 |
| 5'4 | 0,138 | -0,006 | 0,102 | -0,006 | 0,093 | -0,007 |
| 5'5 | 0,041 | -0,007 | 0,088 | -0,012 | 0,088 | -0,002 |

The completed analysis of vertical movements of the cylindrical shell at full loading, 1/2 and 1/3 of the surface portion is illustrated in fig. 17 – 19.

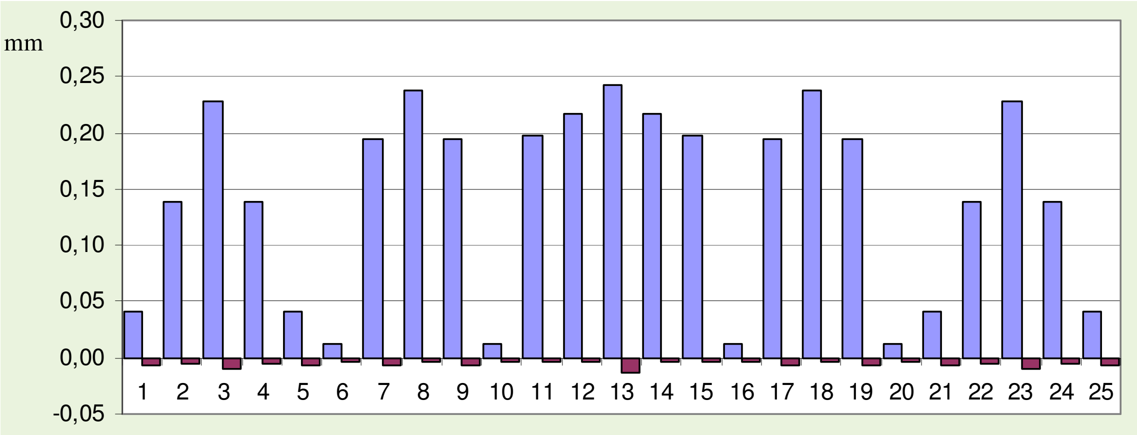


**Figure 17 – Graphical representation of cylindrical shell vertical movements under the evenly distributed load of 10kN/m$^2$ over the entire structure surface**

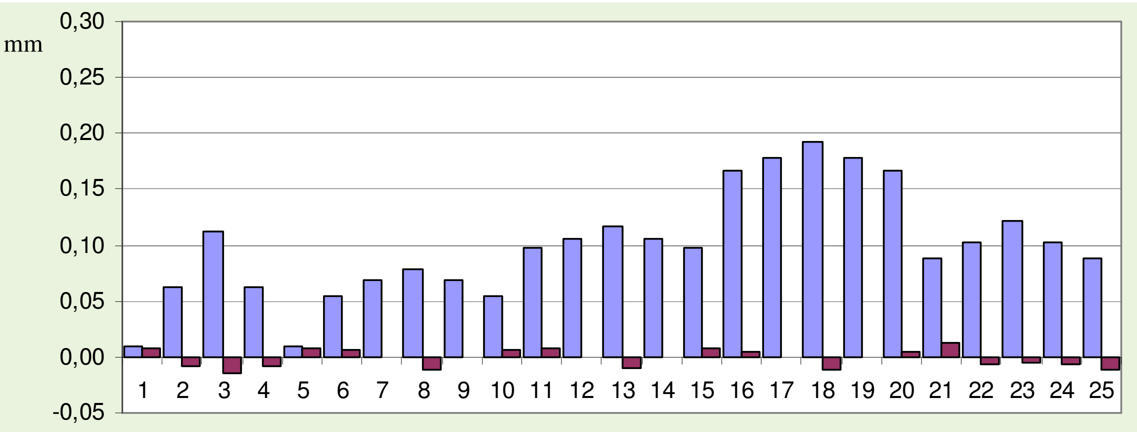


**Figure 18 – Graphical representation of cylindrical shell vertical movements under the evenly distributed load of 10kN/m$^2$ over 1/2 of the structure surface**

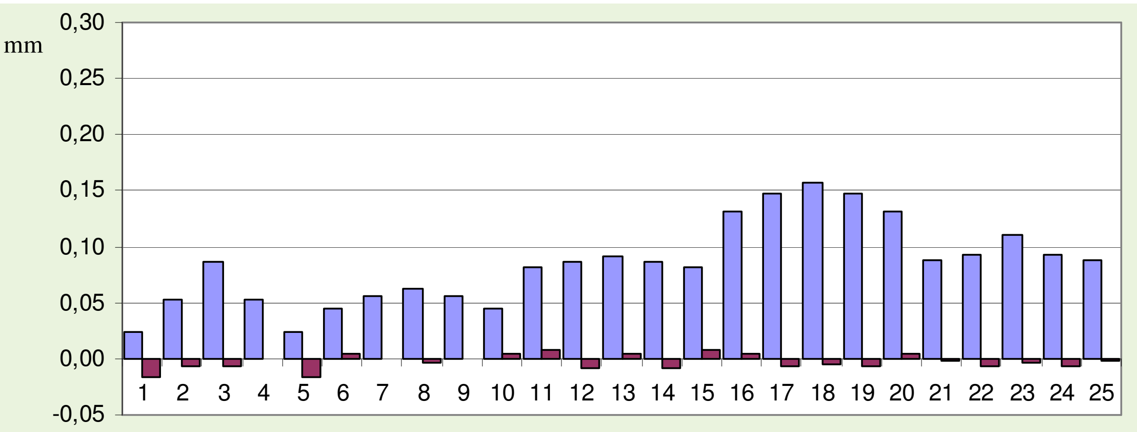


**Figure 19 – Graphical representation of cylindrical shell vertical movements under the evenly distributed load of 10kN/m$^2$ over 1/3 of the structure surface**

**Table 2 – Averaged readings of spherical shell indicators**

| Indicator | Vertical movements (mm) | | | | | | | |
|---|---|---|---|---|---|---|---|---|
| | Full loading | Δ | 1/2 of the surface | Δ | 1/4 of the surface | Δ | 1/8 of the surface | Δ |
| 1 | 0,275 | 0,021 | 0,117 | 0,004 | 0,044 | 0,026 | 0,016 | 0,006 |
| 2 | 0,382 | 0,009 | 0,136 | 0,000 | 0,055 | 0,024 | 0,023 | 0,006 |
| 3 | 0,419 | 0,082 | 0,153 | 0,021 | 0,068 | 0,013 | 0,027 | 0,007 |
| 4 | 0,377 | 0,013 | 0,133 | 0,003 | 0,051 | 0,003 | 0,020 | 0,009 |
| 5 | 0,264 | 0,030 | 0,115 | 0,006 | 0,039 | 0,031 | 0,015 | 0,007 |
| 6 | 0,383 | 0,008 | 0,157 | 0,023 | 0,142 | -0,021 | 0,042 | 0,001 |
| 7 | 0,597 | -0,021 | 0,195 | 0,004 | 0,149 | -0,018 | 0,054 | 0,000 |
| 8 | 0,496 | 0,026 | 0,197 | 0,011 | 0,159 | -0,003 | 0,063 | -0,004 |
| 9 | 0,590 | -0,014 | 0,185 | 0,014 | 0,093 | 0,003 | 0,049 | 0,005 |
| 10 | 0,387 | 0,004 | 0,153 | 0,027 | 0,050 | 0,004 | 0,039 | 0,003 |
| 11 | 0,417 | 0,084 | 0,231 | 0,020 | 0,208 | 0,014 | 0,077 | -0,009 |
| 12 | 0,490 | 0,031 | 0,257 | 0,031 | 0,231 | -0,014 | 0,091 | 0,000 |
| 13 | 0,686 | -0,054 | 0,281 | 0,022 | 0,178 | -0,026 | 0,096 | -0,001 |
| 14 | 0,495 | 0,026 | 0,265 | 0,023 | 0,156 | -0,005 | 0,095 | -0,004 |
| 15 | 0,420 | 0,081 | 0,241 | 0,010 | 0,064 | 0,019 | 0,080 | -0,012 |
| 16 | 0,384 | 0,007 | 0,295 | 0,005 | 0,233 | -0,016 | 0,108 | -0,016 |
| 17 | 0,595 | -0,019 | 0,331 | -0,010 | 0,237 | 0,011 | 0,130 | -0,008 |
| 18 | 0,498 | 0,021 | 0,349 | 0,012 | 0,227 | -0,018 | 0,184 | -0,015 |
| 19 | 0,593 | -0,017 | 0,335 | -0,006 | 0,151 | -0,020 | 0,127 | -0,005 |
| 20 | 0,381 | 0,010 | 0,308 | -0,008 | 0,059 | 0,020 | 0,103 | -0,012 |
| 21 | 0,268 | 0,026 | 0,238 | -0,039 | 0,178 | 0,021 | 0,120 | -0,017 |
| 22 | 0,386 | 0,004 | 0,349 | -0,008 | 0,236 | -0,013 | 0,138 | -0,011 |
| 23 | 0,413 | 0,088 | 0,405 | -0,007 | 0,211 | 0,011 | 0,223 | 0,003 |
| 24 | 0,380 | 0,010 | 0,358 | -0,017 | 0,144 | -0,023 | 0,135 | -0,008 |
| 25 | 0,275 | 0,021 | 0,246 | -0,047 | 0,047 | 0,019 | 0,118 | -0,015 |

Graphical representation of spherical shell vertical movements under the evenly distributed load of 10 kN/m$^2$ over the entire structure surface, 1/2, 1/4, and 1/8 portions of it is given in fig. 20 – 23.

Comparison of theoretical and experimental displacements spherical shell and cylindrical shell is given in the table 3 – 4.

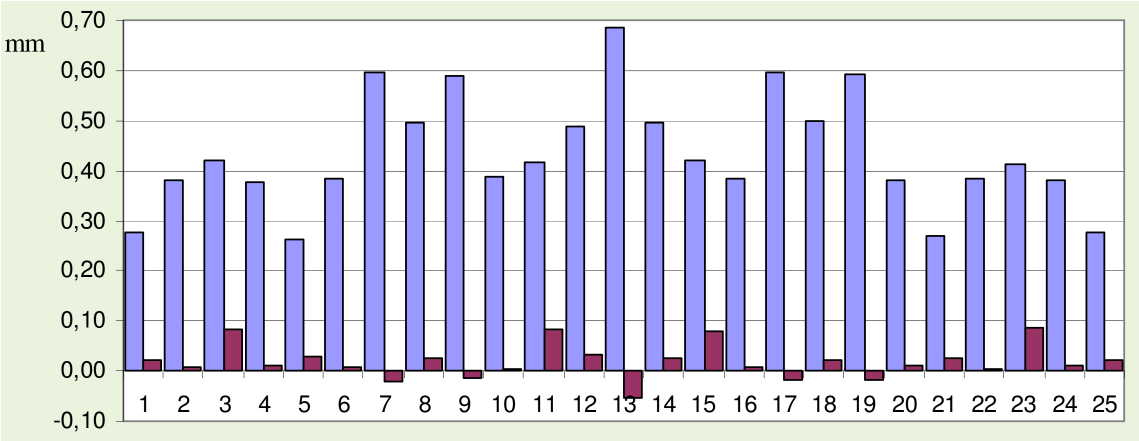


**Figure 20 – Graphical representation of spherical shell vertical movements under the evenly distributed load of 10kN/m$^2$ over the entire structure surface**

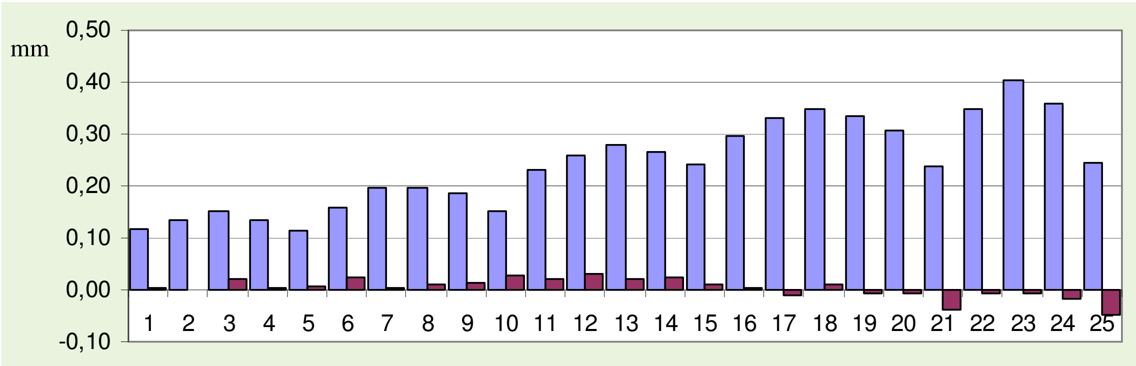


**Figure 21 – Graphical representation of spherical shell vertical movements under the evenly distributed load of 10kN/m$^2$ over 1/2 of the structure surface**

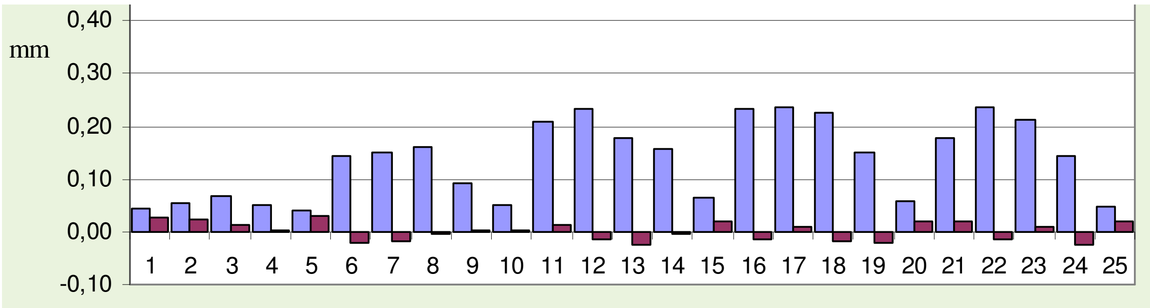


**Figure 22 – Graphical representation of spherical shell vertical movements under the evenly distributed load of 10kN/m$^2$ over 1/4 of the structure surface**

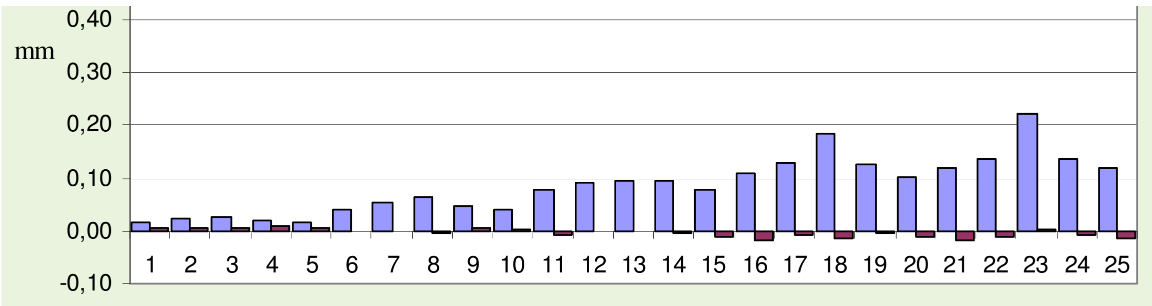


**Figure 23 – Graphical representation of spherical shell vertical movements under the evenly distributed load of 10kN/m$^2$ over 1/8 of the structure surface**

**Table 3 – Comparison of theoretical and research experimental spherical shell**

<table>
<tr><th>Theoretical displacements</th><th>Experimental displacements</th></tr>
<tr><td>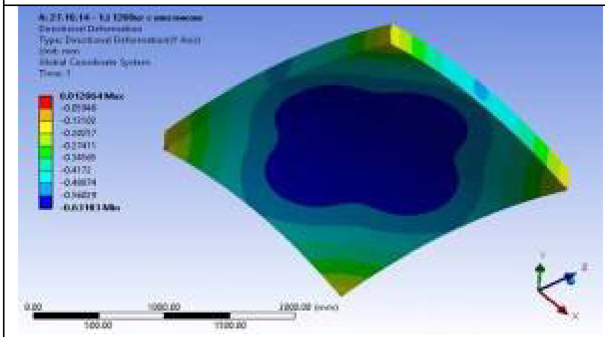</td><td>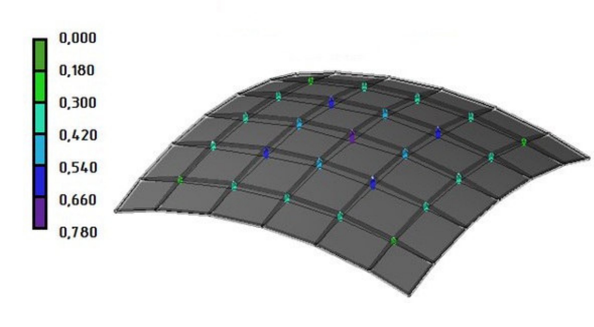
</td></tr>
<tr><td colspan="2">a) over the entire structure surface</td></tr>
<tr><td>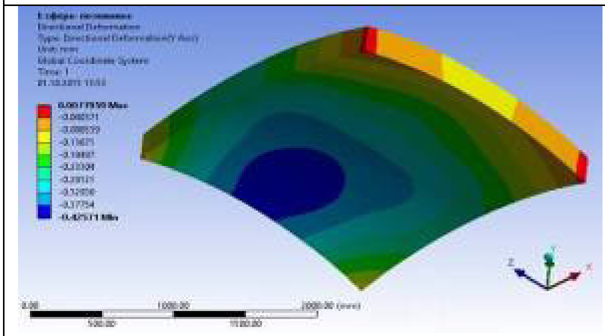</td><td>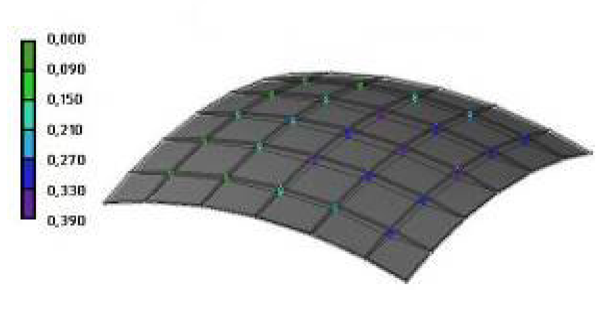
</td></tr>
<tr><td colspan="2">b) over 1/2 of the structure surface</td></tr>
<tr><td>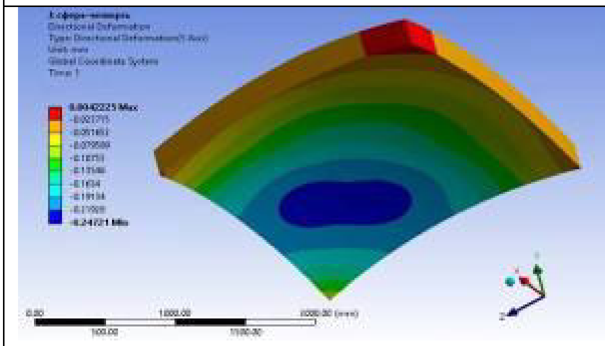</td><td>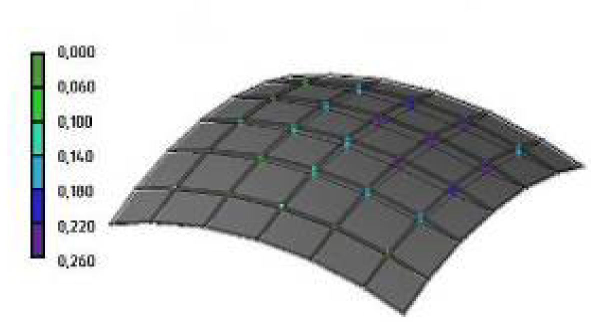
</td></tr>
<tr><td colspan="2">c) over 1/4 of the structure surface</td></tr>
<tr><td>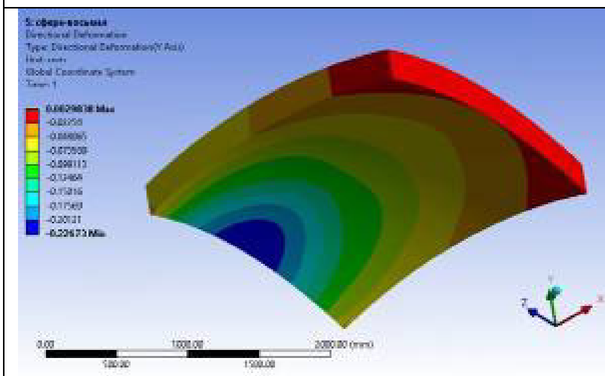</td><td>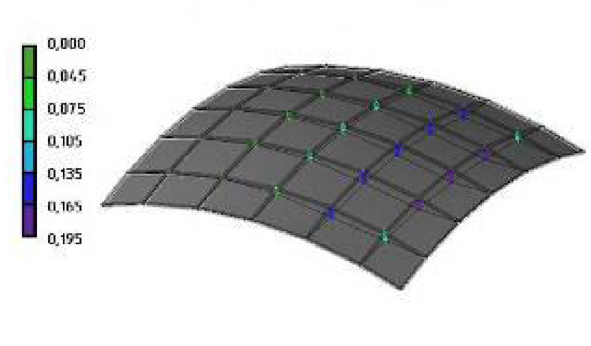
</td></tr>
<tr><td colspan="2">г) over 1/8 of the structure surface</td></tr>
</table>

**Table 4 – Comparison of theoretical and research experimental cylindrical shell**

| **Theoretical displacements** | **Experimental displacements** |
|---|---|
| 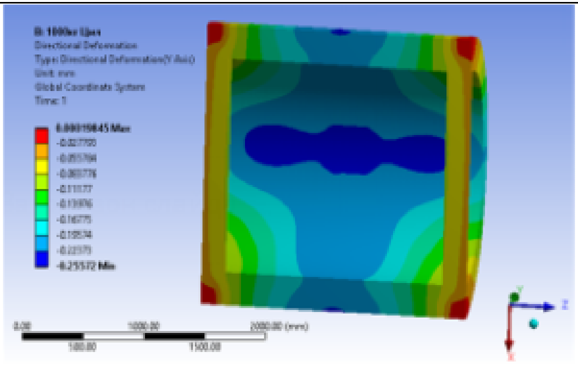 | 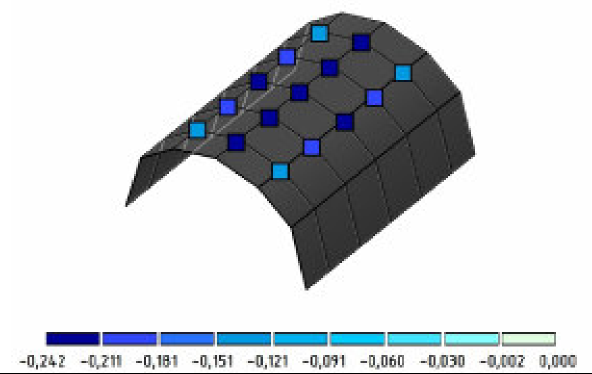 |
| **a) over the entire structure surface** | |
| 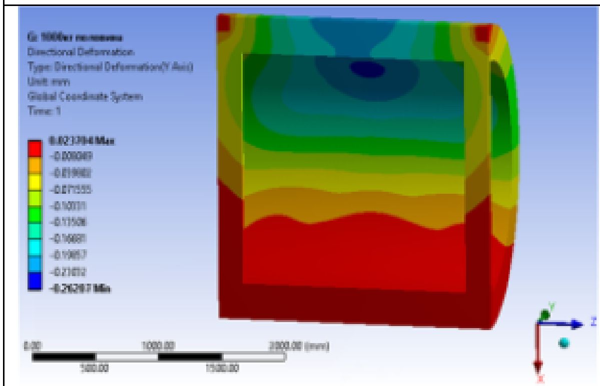 | 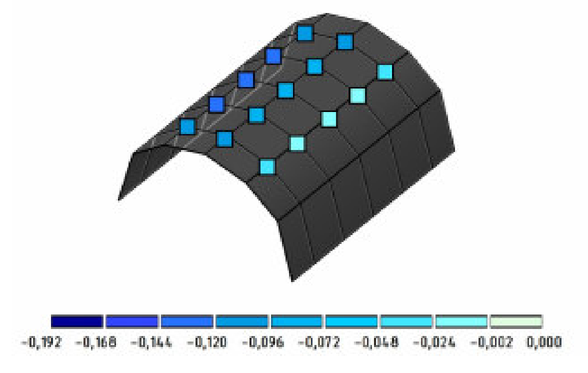 |
| б) **over 1/2 of the structure surface** | |
| 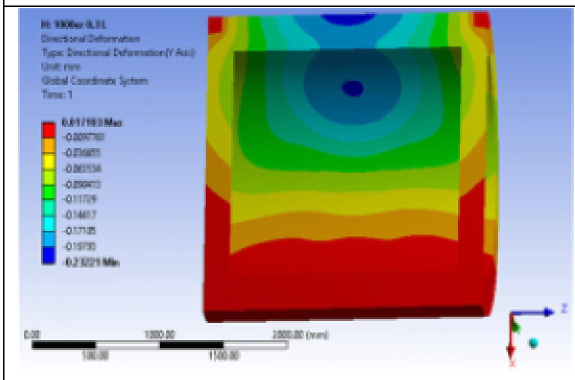 | 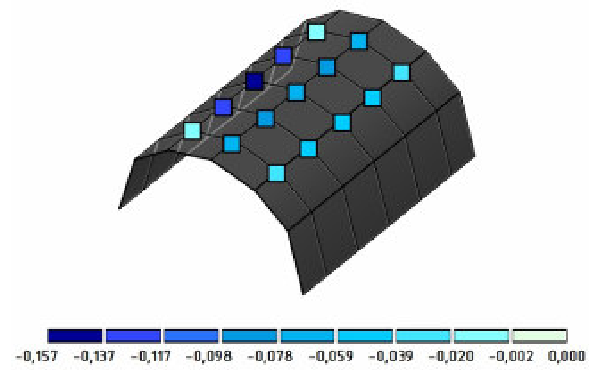 |
| в) **over 1/3 of the structure surface** | |

**Research conclusions, perspectives and further development**. The following research shows that structural elements possess all necessary strength and rigidity properties of bearing members of monolithic reinforced concrete buildings.

In general it should be noted that the completed research defines «Monofant» system representativeness and opens new capabilities of cast-in-place construction that is proved by complex design in Kharkiv (fig. 24).

**Figure24 – Design («Monofant» system)**

***References***

1. *Useful model patent №89464 Ukraine, E 04B 1/B (2006.01) «Momofant» frame building / Shmukler V.S, Babaev V.M., Bugaevsky S.O., Berezhna K.V., Karyakin I.A., Kondraschenko V.I., Sersky I.M. – 2013 11919; application 10.10.2013; publication 25.04.2014. Bulletin №8.*
2. *Babaev V., Shmukler V., Bugayevskiy S., Nikulin V. Cast Reinforced Concrete Frame of Buildings and Methods of Its Erection // Journal of Civil Engineering and Construction. – 2016. – Volume 5. Number 2. – Pp. 143-156. http://www.techrev.org.uk/jcec/5.2/jcec.5.2.143.pdf*
3. *Gaponova L.V., The experimental and theoretical research of stress-strain behaviour of a coating spherical shell [Text] / Gaponova L.V., Kalmikov O.A., Grebenchuk S.S. // Collection of scientific papers of Ukrainian State University of Railway Transport. – 2015. – Issue 157. – p.p. 102-113. http://csw.kart.edu.ua/article/view/61641/57380*
4. *Gaponova L.V., The stress- strain behaviour of the a coating cylindrical shell [Text] / Gaponova L.V., Kalmikov O.A., Grebenchuk S.S. // Municipal infrastructure of cities. – 2016. – Issue. 126. – p.p. 9-18.: http://khg.kname.edu.ua/index.php/khg/article/view/4740/4700*
5. *V. Babaev, V. Shmukler,. S. Grebenchuk, L. Gaponova, L., Kalmikov O. // Analysis of Stress-Strain State of Spherical Roof Shell / 1 st International Conference on Engineering and Innovative Technology, SU-ICEIT 2016, April 12-14, 2016, Salahaddin University-Erbil, Kurdistan, Iraq. http://zancojournals.su.edu.krd/index.php/JPAS/article/view/801/411*
6. *Useful model patent №44125, MPK G01M19/00, G01N3/00, G01M5/00. The device for testing slabs and shells in situ /Shmukler V.S., Chuprinin A.A., Abbasi R. - # u200901598; application 24.02.09; published* 25.09.09, *Bulletin №12.*


Received 02.04.2017